THE JOURNAL OF BIOLOGICAL CHEMISTRY
Vol. 278, No. 8, Issue of February 21, pp. 6291–6300, 2003
Printed in U.S.A.

The GIT Family of Proteins Forms Multimers and Associates with the Presynaptic Cytomatrix Protein Piccolo*

Received for publication, December 3, 2002
Published, JBC Papers in Press, December 6, 2002, DOI 10.1074/jbc.M212287200

Seho Kim‡, Jaewon Ko‡, Hyewon Shin‡, Jae-Ran Lee‡, Chunghun Lim‡, Jin-Hee Han§, Wilko D. Altrock¶, Craig C. Garner‖, Eckart D. Gundelfinger¶, Richard T. Premont, Bong-Kiun Kaang§, and Eunjoon Kim‡ ‡‡**

*From the ‡Department of Biological Sciences, Korea Advanced Institute of Science and Technology, Daejeon 305-701, Korea, the §Molecular Neurobiology Laboratory, Institute of Molecular Biology and Genetics, School of Biological Sciences, College of Natural Sciences, Seoul National University, Seoul 151-742, Korea, the ¶Department of Neurochemistry and Molecular Biology, Leibniz Institute for Neurobiology, Brenneckestr. G, D-39118 Magdeburg, Germany, the ‖Department of Psychiatry and Behavioral Sciences, Nancy Pritzker Laboratory, Stanford University, Stanford, California 94305-5485, and the **Department of Medicine (Gastroenterology), Duke University Medical Center, Durham, North Carolina 27710*

The cytoskeletal matrix assembled at active zones (CAZ) is implicated in defining neurotransmitter release sites. However, little is known about the molecular mechanisms by which the CAZ is organized. Here we report a novel interaction between Piccolo, a core component of the CAZ, and GIT proteins, multidomain signaling integrators with GTPase-activating protein activity for ADP-ribosylation factor small GTPases. A small region (~150 amino acid residues) in Piccolo, which is not conserved in the closely related CAZ protein Bassoon, mediates a direct interaction with the Spa2 homology domain (SHD) domain of GIT1. Piccolo and GIT1 colocalize at synaptic sites in cultured neurons. In brain, Piccolo forms a complex with GIT1 and various GIT-associated proteins, including βPIX, focal adhesion kinase, liprin-α, and paxillin. Point mutations in the SHD of GIT1 differentially interfere with the association of GIT1 with Piccolo, βPIX, and focal adhesion kinase, suggesting that these proteins bind to the SHD by different mechanisms. Intriguingly, GIT proteins form homo- and heteromultimers through their C-terminal G-protein-coupled receptor kinase-binding domain in a tail-to-tail fashion. This multimerization enables GIT1 to simultaneously interact with multiple SHD-binding proteins including Piccolo and βPIX. These results suggest that, through their multimerization and interaction with Piccolo, the GIT family proteins are involved in the organization of the CAZ.

The active zone is a specialized presynaptic plasma membrane region where synaptic vesicles dock and fuse (1). The cytoskeletal matrix (cytomatrix) assembled at active zones (CAZ)[1] is a complex proteinaceous structure implicated in organizing the site of neurotransmitter release (2, 3). Recent studies have identified several core CAZ components involved in orchestrating the formation and functions of the CAZ: Piccolo/aczonin (4–6), Bassoon (7), RIM (8), Munc13 (9), and CAST/ERC (10, 11).

Piccolo is a large (~530 kDa) CAZ protein that is spatially restricted to active zones within the nerve terminal (4–6). Through its two zinc fingers, Piccolo interacts with the prenylated Rab acceptor 1 (5), a small (185 aa) soluble protein known to bind regulators of endo- and exocytosis, including Rab3, Rab5, and VAMP2/synaptobrevin II (12). A proline-rich sequence of Piccolo binds the actin cytoskeleton regulator profilin (6). In addition, the C_2A domain of Piccolo mediates homodimerization and heterodimerization with RIM (13). Intriguingly, Piccolo associates with an ~80-nm dense core granulated vesicle (termed Piccolo transport vesicle) that contains other active zone components, suggesting that Piccolo and related active zone components are transported to nascent synapses as a preassembled package for the rapid and efficient formation of active zones (14). Although Piccolo's size, domain structure, and association with an active zone precursor vesicle suggest that it may be an important organizer of the CAZ, little is known about the mechanism by which this organization is carried out.

GIT1 was originally isolated as a protein interacting with G-protein-coupled receptor kinases (15). The GIT family of proteins contains two known members, GIT1/Cat-1/p95-APP1 and GIT2/Cat-2/PKL/p95-APP2/KIAA0148 (15–22). GIT proteins contain a GTPase-activating protein (GAP) domain for ADP-ribosylation factors (ARFs), small GTP-binding proteins implicated in the regulation of membrane traffic, and the actin cytoskeleton (23). In addition, GIT proteins contain various domains for protein interactions, including ankyrin repeats, the Spa2 homology domain (SHD), and the G-protein-coupled receptor kinase-binding domain (GRKBD). GIT proteins regulate endocytosis of various membrane proteins (15, 24) and regulate the assembly of focal adhesion complexes by interacting with the Rho-type guanine nucleotide exchange factor (GEF) βPIX, focal adhesion kinase (FAK), and the focal adhesion adaptor protein paxillin (16, 18, 25). However, neuronal

* This work was supported by grants from the Korean Ministry of Science and Technology, the Korea Science and Engineering Foundation, the Korea Research Foundation (to E. K.), the National Research Laboratory (Grant M1-0104-00-0140) (to B. K. K.), and the Deutsche Forschungsgemeinschaft (SFB426/A1) (to E. D. G.) and by National Institutes of Health Grants RO1-NS39471 and PO1-AG06569 (to C. C. G.). The costs of publication of this article were defrayed in part by the payment of page charges. This article must therefore be hereby marked "*advertisement*" in accordance with 18 U.S.C. Section 1734 solely to indicate this fact.

‡‡ To whom correspondence should be addressed: Tel.: 42-869-2633; Fax: 42-869-2610; E-mail: kime@mail.kaist.ac.kr.

[1] The abbreviations used are: CAZ, cytoskeletal matrix assembled at active zones; GRKBD, G-protein-coupled receptor kinase-binding domain; GAP, GTPase-activating protein; ARF, ADP-ribosylation factor; SHD, Spa2 homology domain; GEF, guanine nucleotide exchange factor; FAK, focal adhesion kinase; EGFP, enhanced green fluorescent protein; aa, amino acid(s); CMV, cytomegalovirus; GST, glutathione *S*-transferase; PBS, paxillin-binding subdomain; GBD, GIT-binding domain; RU, resonance units; DIV, days *in vitro*; EM, electron microscopy; hemagglutinin.

functions of GIT proteins, despite their widespread tissue expression, including the brain (15, 19), remained unknown.

Here we report that Piccolo directly interacts with GIT and various GIT-associated proteins. Moreover, GIT proteins form homo- and heteromultimers, which enable GIT proteins to form a ternary complex with Piccolo and βPIX. These results suggest that GIT proteins participate in the organization of the CAZ.

EXPERIMENTAL PROCEDURES

Yeast Two-hybrid Assay—A yeast two-hybrid assay was performed as previously described (26). HIS3 growth and β-galactosidase activity were measured semi-quantitatively. For yeast two-hybrid screen, the full-length GIT1 (aa 1–770) was amplified by PCR from pBK(Δ) GIT1 (15) and subcloned into pBHA (a bait vector containing LexA DNA-binding domain) digested with *Eco*RI. Regions of Piccolo (aa 2197–2350) and βPIX (aa 440–646) were subcloned into the *Eco*RI-*Bam*HI site of pBHA. The *Eco*RI site of GIT2 long and GIT2 short in pBK(Δ) GIT2 long and pBK(Δ) GIT2 short (KIAA0148) was removed by site-directed mutagenesis without changing amino acids, and GIT2 long and GIT2 short were subcloned into the *Eco*RI site of pBHA. The following regions of GIT1 and Piccolo were subcloned into the *Bam*HI-*Eco*RI site of pGAD10: GIT1, aa 1–129, 1–244, 1–336, 1–374, 130–244, 130–374, 245–374, 375–528, 375–645, 405–485, 486–645, 486–770, and 646–770; Piccolo, aa 2011–2196, 2011–2350, 2197–2350, 2197–2468, and 2344–2468. Full-length GIT1 (aa 1–770) and GIT1 GRKBD (aa 375–770) were subcloned into the *Eco*RI site of pGAD10. Full-length GIT2 long (aa 1–759) was subcloned into the *Eco*RI site of pGAD10. Bassoon (aa 1730–2237) was amplified by PCR from pCMV2-RBB29 (aa 1630–3264 of rat Bassoon) and subcloned into pGAD10 digested with *Bam*HI and *Eco*RI. For pGAD10 GIT1 aa 1–374 Δ (273–303), GIT1 aa 1–272 and 304–374 were amplified by PCR, digested with *Bam*HI-*Kpn*I and *Kpn*I-*Eco*RI, respectively, and subcloned into the *Bam*HI-*Eco*RI site of pGAD10. GIT1 (aa 1–374 and 1–770) with mutations in the SHD (F285A, L288A, R298A, and R299A) were amplified by PCR from pBK(Δ) GIT1 mutants and subcloned into the *Bam*HI-*Eco*RI (for aa 1–374) or *Eco*RI (for aa 1–770) sites of pGAD10.

GST Pull-down Assay—For GST fusion protein constructs, the following regions of Piccolo and GIT1 were subcloned into *Bam*HI-*Eco*RI site of pGEX-4T-1 (Amersham Biosciences): Piccolo (aa 2011–2350); GIT1, GAP-SHD (aa 1–374), CC (aa 405–485), SP (aa 486–645), and PBS (aa 646–770). GIT1 GRKBD (aa 375–770) was subcloned into the *Eco*RI site of pGEX-4T-1. For H6 fusion protein constructs, GIT1 GAP-SHD (aa 1–374) was subcloned into pRSET A (Invitrogen) digested with *Bam*HI and *Eco*RI, and GIT1 GRKBD (aa 375–770) and GIT1 full-length (aa 1–770) into the *Eco*RI site of pRSET B (Invitrogen). EGFP-GIT1 deletion constructs were generated by subcloning the following regions of GIT1 into pEGFP-C1 (Clontech): GAP (aa 1–129), ankyrin repeats (aa 130–254), SHD (aa 255–374), and GAP-SHD (aa 1–374) (*Eco*RI and *Bam*HI site); GRKBD (aa 375–770) and GIT1 full-length (aa 1–770) (*Eco*RI site). FLAG-tagged GIT1, GIT2 long, GIT2 short, and PAPα in pBK(Δ) were previously described (15, 19). The GIT-binding domain (GBD, aa 486–566) of βPIX-a was subcloned into the *Eco*RI-*Bam*HI site of pEGFP-C1 (Clontech). For pull-down assay, transfected HEK293T cells were extracted with binding buffer (phosphate-buffered saline with 1% Triton X-100) containing protease inhibitors at 4 °C for 30 min. After centrifugation, the extracts were mixed with GST fusion proteins and incubated for 30 min, followed by precipitation with glutathione-Sepharose 4B resin (Amersham Biosciences). H6-GIT1 fusion proteins were pulled down by the same method. The precipitates were analyzed by immunoblotting with EGFP and His antibodies.

Surface Plasmon Resonance Measurements—H6-GIT1 GAP-SHD and H6-Piccolo were used as ligand and analyte, respectively. For H6-Piccolo, Piccolo (aa 2011–2350) was subcloned into the *Bam*HI and *Eco*RI site of pRSET A (Invitrogen). 177 resonance units (RU) of H6-GIT1 GAP-SHD was immobilized on a CM5 sensor chip (BIAcore) by amine coupling. H6-Piccolo at different concentrations was injected at a flow rate of 10 μl/min. Surface plasmon resonance was monitored by a BIAcore X instrument (BIAcore). HBS (10 mM HEPES, pH 7.4, 150 mM NaCl, 3.4 mM EDTA, 0.005% (v/v) surfactant P20) was used as running buffer. The surface of the sensor chips was regenerated by 1-min injections of 25 mM NaOH at 10 μl/min. All experiments were performed at 25 °C. Data were analyzed using BIAevaluation software 3.1 (BIAcore).

Coimmunoprecipitation Assay—EGFP-Piccolo was constructed by subcloning aa 2011–2350 of Piccolo into pcDNA3 (Invitrogen) digested with *Bam*HI and *Eco*RI, followed by elution of the insert with *Kpn*I and *Xba*I enzymes and subcloning into pEGFP-C1 (Clontech). GIT1 ΔPBS (aa 1–645) was subcloned into the *Bam*HI-*Eco*RI site of pBK(Δ). For GIT1 ΔCC-FLAG, GIT1 aa 1–431 and GIT1 aa 484–770 were amplified by PCR, digested with *Bam*HI-*Kpn*I and *Kpn*I-*Eco*RI, respectively, and subcloned into pBK(Δ) digested with *Bam*HI and *Eco*RI. Myc-tagged βPIX has been described previously (27). Expression constructs of full-length GIT1 (pBK(Δ) GIT1-FLAG) with point mutations in the SHD (F285A, L288A, R298A, and R299A) were generated using a QuikChange site-directed mutagenesis kit (Stratagene). For immunoprecipitation, transfected HEK293T cells were extracted with binding buffer and incubated with M2 FLAG-agarose (Sigma) at 4 °C for 4 h or antibodies against Piccolo (1203, 1:250) or Myc (2 μg/ml) followed by protein A-Sepharose (Amersham Biosciences) precipitation. *In vivo* coimmunoprecipitation was performed as previously described (28). Briefly, the crude synaptosomal fraction of adult rat brain was solubilized with DOC buffer (50 mM Tris-HCl, 1% sodium deoxycholate, pH 9.0), dialyzed against binding/dialysis buffer (50 mM Tris-HCl, 0.1% Triton X-100, pH 7.4), and centrifuged. The supernatant was incubated with Piccolo antibodies (1203, 1:250) or boiled antibodies (negative control) at 4 °C for 2 h, with protein A-Sepharose for additional 2 h, followed by immunoblot analysis of the precipitates with GIT1 (du139, 1:2000), Piccolo (1203, 1 μg/ml), βPIX (1:1000), FAK (1:200), paxillin (1:1000), liprin-α (1120, 0.5 μg/ml), GRIP1 (43–8, 1:1000), vinculin (1:1000), and synaptophysin (1:1000) antibodies.

Sucrose Density Gradient Sedimentation Analysis—H6-GIT1 full-length and H6-GIT1 GAP-SHD fusion proteins were purified and dialyzed against HEPES buffer (10 mM HEPES, pH 7.4, 150 mM NaCl, 0.1% Triton X-100). 200 μl of each fusion protein or molecular weight standards were laid on top of 4 ml of 15–30% linear sucrose density gradient prepared in HEPES buffer containing 10% glycerol and 1 mM dithiothreitol, and centrifuged at 40,000 rpm in an SW41 rotor (Beckman) at 4 °C for 20 h. Molecular mass standards included bovine serum albumin (67 kDa, Sigma), catalase (232 kDa, Sigma), and thyroglobulin (670 kDa, Sigma). After centrifugation, fractions were collected from the top and analyzed by immunoblotting with His antibodies. Molecular weight standards were visualized by Coomassie Brilliant Blue staining.

Antibodies—Rabbit polyclonal GIT1 antibodies (1176) were raised using H6-GIT1 (aa 375–770) as immunogen.[2] Polyclonal Piccolo antibodies were generated in guinea pigs (1203) with H6-Piccolo (aa 2011–2350). The following antibodies have been previously described: rabbit polyclonal GIT1 antiserum (du139) (15), EGFP (1167) (29), liprin-α (1120),[2] and βPIX (27). Guinea pig polyclonal Piccolo antibodies (gp-α-44a-GST-affi) were affinity-purified as described (30). GRIP1 43–8 antibody was a gift from Dr. Pann-Ghill Suh (Pohang University of Science and Technology, Korea). The following antibodies were purchased from commercial sources: FLAG (M2, Sigma), vinculin (Sigma), His (His-probe, H-15, Santa Cruz Biotechnology), paxillin (Transduction Laboratories), FAK (clone 4.47, Upstate Biotechnology), synaptophysin (Sigma), synaptotagmin (Sigma), Myc (9E10, Santa Cruz Biotechnology), and HA (clone 12CA5, Roche Applied Science).

Primary Neuron Culture and Immunostaining—Primary hippocampal neurons were prepared from E18 embryonic rat brains as previously described (31) and maintained in the neurobasal medium (Invitrogen) supplemented with B27 (Invitrogen), 0.5 mM glutamine, and 12.5 μM glutamate. At 21 days *in vitro* (DIV), hippocampal neurons were fixed and permeabilized with precooled methanol at −20 °C for 20 min and incubated with primary antibodies, Piccolo (gp-α-44a-GST-affi, 1:1000) and GIT1 (1176, 2 μg/ml), followed by Cy3- or fluorescein isothiocyanate-conjugated secondary antibodies (1:250 and 1:100, respectively, Jackson ImmunoResearch). Images were captured by confocal laser scanning microscopy (LSM510, Zeiss).

RESULTS

Characterization of the Interaction between Piccolo and the GIT Family Proteins in the Yeast Two-hybrid Assay—We identified the interaction between Piccolo and GIT1 by yeast two-hybrid screen of a rat brain cDNA library using the full-length GIT1 as bait. One of the positive clones was a fragment of Piccolo (aa 2011–2468). By deletion analysis, a minimal GIT-binding domain in Piccolo was narrowed down to the middle third of the positive clone (aa 2197–2350, ~150 aa residues), excluding the C-terminal proline-rich region (Fig. 1*A*). Conversely, a minimal Piccolo-binding region in GIT1 was defined as the SHD (Fig. 1*B*), a domain known to mediate the associ-

[2] J. Ko, S. Kim, J. G. Valtschanoff, H. Shin, J. R. Lee, M. Sheng, R. T. Premont, R. Weinberg, and E. Kim. (2003) *J. Neurosci*. In press

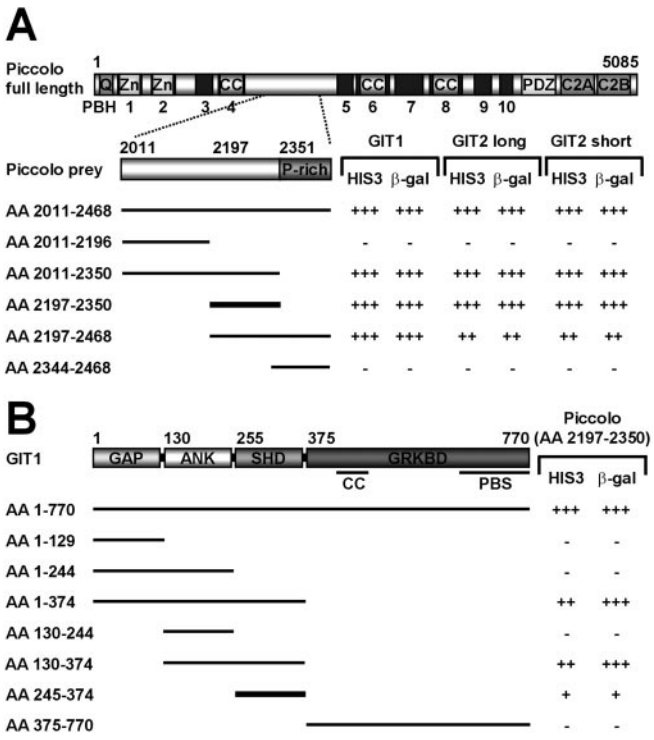

FIG. 1. **Characterization of the interaction between Piccolo and the GIT family in the yeast two-hybrid assay.** *A*, deletions of the Piccolo-positive clone in the pGAD10 prey vector were tested for binding to GIT1 (full-length), GIT2 long, and GIT2 short in the pBHA bait vector in a yeast two-hybrid assay. The Piccolo Bassoon homology (*PBH*) domains are indicated by the *numbers underneath* the *diagram* of full-length Piccolo. *Q*, glutamine heptad repeats; *Zn*, Zinc finger; *CC*, coiled coil; *PDZ*, PSD-95/Dlg/ZO-1 domain; *C2*, C2 domain. *Small numbers* refer to aa residues at the boundaries of the domains or full-length proteins. *P-rich*, proline-rich region. HIS3 activity: +++ (>60%), ++ (30–60%), + (10–30%), − (no significant growth); β-galactosidase: +++ (<45 min), ++ (45–90 min), + (90–240 min), − (no significant β-galactosidase activity). *B*, deletions of GIT1 in pGAD10 were tested for their binding against Piccolo (aa 2197–2350). The SHD of GIT1 mediates the association with Piccolo. *GAP*, ARF GAP domain; *ANK*, ankyrin repeats; *SHD*, Spa2 homology domain; *GRKBD*, G-protein-coupled receptor kinase-binding domain; *CC*, coiled coil; *PBS*, paxillin-binding subdomain.

ation of GIT1 with βPIX and FAK (25). In addition to GIT1, Piccolo interacted with GIT2 long (full-length), which shares the same domain structure with GIT1 (19), as well as GIT2 short, a splice variant of GIT2 that lacks most of the C-terminal GRKBD but contains the SHD (19) (Fig. 1*A*) (see Fig. 2*D* for the structural organization of GIT2 splice variants). In contrast, a region of Bassoon (aa 1730–2237) that corresponds to the Piccolo prey clone (aa 2011–2468) showed no significant homology to the minimal GIT-binding domain of Piccolo (aa 2197–2350), and did not interact with GIT1, GIT2 long, or GIT2 short (data not shown). This indicates that the GIT proteins selectively interact with Piccolo and suggests that Piccolo and Bassoon, two closely related CAZ proteins known to colocalize in synapses (5), may have differential functions.

Characterization of the Interaction between Piccolo and GIT Proteins by Pull-down Assays and Surface Plasmon Resonance Measurements—As an independent assay to characterize the interaction of Piccolo with GIT proteins, we performed GST pull-down assays using GST-Piccolo (aa 2011–2350) and HEK293T cell lysates transfected with EGFP-tagged GIT1 deletions (Fig. 2, *A* and *B*). Consistent with the yeast-two hybrid results (Fig. 1*B*), GST-Piccolo, but not GST alone, selectively pulled down EGFP-tagged GIT1 deletions containing the SHD (Fig. 2*B*), indicating that the SHD of GIT1 mediates its interaction with Piccolo. In addition, GST-Piccolo selectively pulled down H6-GIT1 GAP-SHD (aa 1–374) but not H6-GIT1 GRKBD (aa 375–770) fusion proteins (Fig. 2*C*), indicating that Piccolo directly interacts with GIT1. We further performed pull-down assays on HEK293T cell lysates transfected with FLAG-tagged full-length GITs (GIT1-FLAG, GIT2 long-FLAG, and GIT2 short-FLAG) and an unrelated protein with the ARF GAP domain, PAPα/PAG3, which lacks the SHD (32), as control (Fig. 2*D*). GST-Piccolo brought down GIT1, GIT2 long, and GIT2 short but not PAPα/PAG3, consistent with the yeast two-hybrid results (Fig. 1*A*), indicating that Piccolo selectively interacts with the GIT family proteins. The relatively inefficient pull-down of GIT2 short by GST-Piccolo differs from the yeast two-hybrid results (Fig. 1*A*). This could be due to differences in the assay, but both assays (yeast two-hybrid and pull-down) clearly showed that GIT2 short can bind Piccolo.

To determine the affinity and stoichiometry of the interaction between Piccolo and GIT1, we performed surface plasmon resonance experiments. H6-Piccolo (analyte) in running buffer specifically bound to the H6-GIT1 GAP-SHD (ligand) immobilized on the sensor chip. The plot of R_{eq} (response at the steady state) against the concentration of H6-Piccolo gave a dissociation constant of 14.5 μM and an R_{max} (maximum binding capacity of the surface ligand) of 142 RU (Fig. 2*E*). Considering that the RU of immobilized H6-GIT1 GAP-SHD is 177, the molar ratio of H6-Piccolo to H6-GIT1 GAP-SHD is ~0.9, indicating that the GIT1 SHD has one binding site for Piccolo. The relatively low affinity of the Piccolo-GIT interaction in this assay may result from, in contrast to full-length GIT1, the GAP-SHD region of GIT1 showing a relatively low apparent affinity for Piccolo in the yeast two-hybrid assay (Fig. 1*B*) and pull-down assay (Fig. 2*B*). Another explanation may be that immobilization of H6-GIT1 GAP-SHD on the CM5 sensor chip by amine coupling might have modified arginine residues in the GIT1 SHD that appear to be important for binding to Piccolo (see Fig. 5 for further details).

Piccolo and GIT1 Colocalize at Synaptic Sites in Cultured Neurons—To determine whether Piccolo and GIT1 colocalize in subcellular regions of neurons, we performed double-label immunofluorescence staining on cultured hippocampal neurons after 21 days *in vitro* (DIV) (Fig. 3). Consistent with the reported presynaptic localization of Piccolo (5), Piccolo was primarily localized at discrete punctate structures located along neurites (Fig. 3*B*). GIT1 displayed a much wider distribution than Piccolo, and the immunoreactivity was found associated with a number of small intracellular structures scattered throughout the neurons (Fig. 3*A*). Importantly, however, several of the GIT1-positive structures, presumably representing synaptic GIT1 proteins, colocalized with the Piccolo puncta. The GIT1 puncta that do not overlap with Piccolo appear to be extrasynaptic GIT1 proteins, as evidenced by immunohistochemical and biochemical results.[2] These results suggest that GIT1 proteins are widely distributed to both synaptic as well as non-synaptic sites and that presynaptic GIT1 proteins colocalize with Piccolo.

Piccolo and GIT1 Form a Complex in Heterologous Cells and Brain—We then examined in a series of coimmunoprecipitation experiments whether interaction between Piccolo and GIT1 occurs on a cellular level (Fig. 4, *A* and *B*). Incubation of HEK293T cell lysates doubly transfected with EGFP-tagged Piccolo (EGFP-Piccolo, aa 2011–2350) and GIT1-FLAG (full-length) with FLAG antibodies immunoprecipitated GIT1-FLAG and coprecipitated EGFP-Piccolo (Fig. 4*A*). In control experiments, FLAG antibodies did not bring down EGFP-Piccolo from singly transfected cells. In inversely designed coimmunoprecipitation experiments Piccolo antibodies

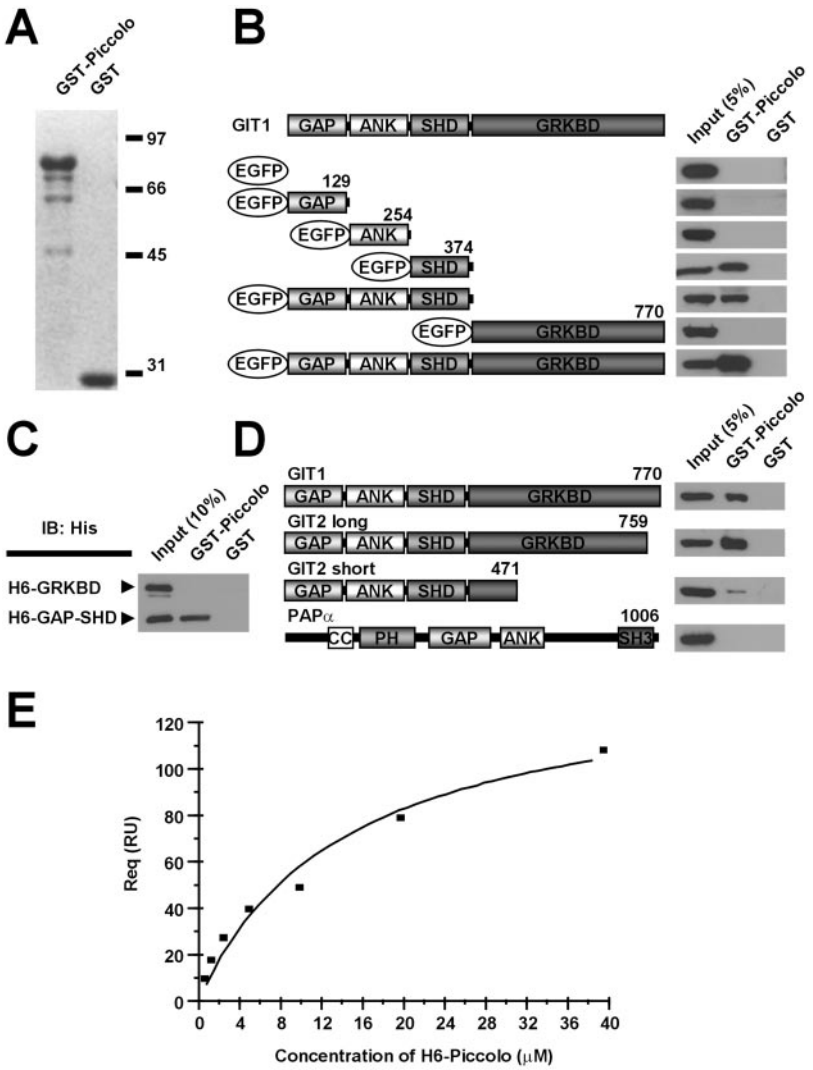

FIG. 2. **Characterization of the interaction between Piccolo and GIT proteins by the pull-down assay and surface plasmon resonance measurements.** *A* and *B*, HEK293T cell lysates transiently transfected with EGFP-tagged deletions of GIT1 were pulled down by equal amounts (5 μg) of GST-Piccolo (aa 2011–2350) or GST alone, and analyzed by immunoblotting with EGFP antibodies. GST fusion proteins used in the pull-down assay were visualized by Coomassie Brilliant Blue staining (*A*). *C*, H6-GIT1 GAP-SHD (aa 1–374) and H6-GIT1 GRKBD (aa 375–770) fusion proteins (1 μg) were pulled down by GST-Piccolo, or GST alone (2 μg), and analyzed by immunoblotting with His antibodies. *IB*, immunoblotting. *D*, HEK293T cell lysates transfected with FLAG-tagged full-length GITs (GIT1-FLAG, GIT2 long-FLAG, and GIT2 short-FLAG) or PAPα/PAG3 (an unrelated ARF GAP) were pulled down by GST-Piccolo or GST alone (5 μg) and analyzed by immunoblotting with FLAG antibodies. *PH*, pleckstrin homology domain; *SH3*, Src homology 3 domain. *E*, the affinity and stoichiometry of the Piccolo-GIT1 interaction determined by surface plasmon resonance measurements. H6-Piccolo was perfused over the H6-GIT1 GAP-SHD immobilized on a CM5 sensor chip. Responses at the steady state (*Req*) were plotted against the concentration of H6-Piccolo and analyzed by non-linear curve fitting.

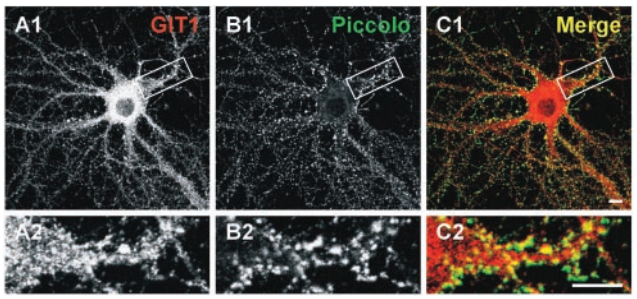

FIG. 3. **Piccolo and GIT1 colocalize at synaptic sites in cultured neurons.** Cultured hippocampal neurons (DIV 21) were labeled by double-immunofluorescence staining with GIT1 (1176) and Piccolo (gp-α-44a-GST-affi) antibodies. GIT1 (*A1*, *red*) distributes to a number of small intracellular structures scattered throughout the neurons, and several of the GIT1-positive structures colocalize with presynaptic Piccolo puncta (*B1*, *green*). *C1* and *C2* are *merged images*. *A2*, *B2*, and *C2* represent enlargement of the *boxes* in *A1*, *B1*, and *C1*, respectively. *Scale bar*: 10 μm.

immunoprecipitated EGFP-Piccolo and coprecipitated GIT1-FLAG (Fig. 4*B*).

To determine whether Piccolo and GIT1 form a complex in brain, we performed coimmunoprecipitation experiments on rat brain extracts (Fig. 4*C*). Immunoprecipitation on detergent lysates of the crude synaptosomal fraction of adult rat brain with Piccolo antibodies precipitated Piccolo and coprecipitated GIT1 and various proteins that are known to associate with GIT1, including βPIX (16, 18, 25), FAK (25), paxillin (18), liprin-α,[2] and the liprin-α-associated GRIP1 (33) but not vinculin and synaptophysin (negative control). The multiple bands in the βPIX immunoblot represent the splice variants of βPIX expressed in the brain (34, 35). Immunoprecipitation with boiled Piccolo antibodies did not bring down any of the above proteins. These results indicate that Piccolo associates with GIT1 and GIT1-associated proteins *in vivo*.

Piccolo, βPIX, and FAK Bind to the SHD of GIT1 by Different Mechanisms—The GIT1 SHD contains two highly conserved repeats that are ~30 aa residues in length (Fig. 5*A*, *diagram* in Fig. 5*B*). Using a yeast two-hybrid assay, we examined whether both repeats were required for binding to Piccolo or βPIX. We found that deletion of either repeat 1 or repeat 2 from the aa 1–374 GIT1 backbone eliminated its interaction with Piccolo and βPIX (Fig. 5*B*), suggesting both repeats of the SHD are required for binding to SHD ligands. This is consistent with the 1:1 stoichiometry of the Piccolo-GIT1 interaction obtained from the surface plasmon resonance results (Fig. 2*E*).

Multiple aa sequence alignment of the repeats in the SHD from GITs of various species and yeast Spa2p revealed that there are four invariant residues in each repeat; Phe, Leu, Arg, and Arg (Fig. 5*A*, indicated by *arrowheads*). To determine whether any of these amino acids were important for Piccolo binding, these residues in the first repeat of the GIT1 SHD were mutated into alanines (F285A, L288A, R298A, and R299A). When these mutations were introduced into the aa

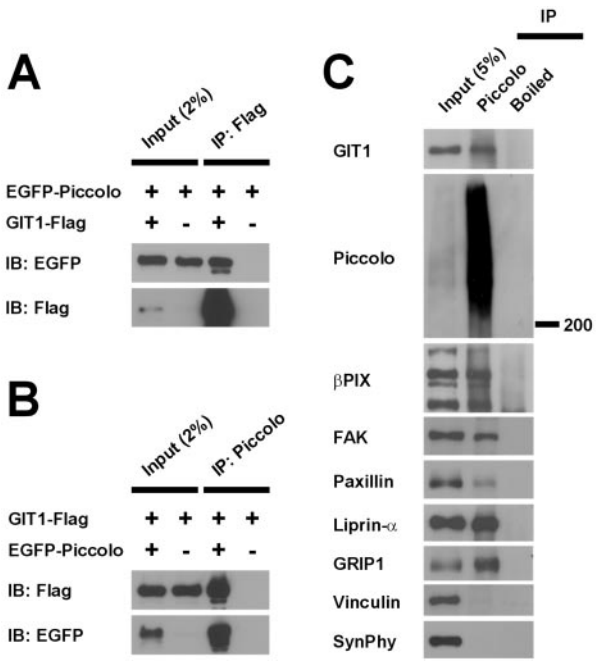

FIG. 4. **Piccolo forms a complex with GIT1 in heterologous cells and brain.** *A*, HEK293T cell lysates doubly transfected with EGFP-tagged Piccolo (EGFP-Piccolo, aa 2011–2350) plus GIT1-FLAG (full-length), or EGFP-Piccolo alone, were immunoprecipitated with FLAG antibodies, and analyzed by immunoblotting with EGFP and FLAG antibodies. *IP*, immunoprecipitation. *B*, HEK293T cell lysates doubly transfected with EGFP-Piccolo plus GIT1-FLAG, or GIT1-FLAG alone, were immunoprecipitated with Piccolo (1203) antibodies and analyzed by immunoblotting with FLAG and EGFP antibodies. *C*, detergent lysates of the crude synaptosomal fraction of adult rat brain were immunoprecipitated with Piccolo (1203) antibodies (untreated or boiled) and analyzed by immunoblotting with GIT1, Piccolo, βPIX, FAK, paxillin, liprin-α, GRIP1, vinculin, and synaptophysin (*SynPhy*) antibodies. *200*, 200-kDa molecular mass marker.

1–374 GIT1 backbone and tested in the yeast two-hybrid assay, we found that the L288A mutation abolished GIT1-Piccolo interactions (Fig. 5*B*). The other mutations also significantly reduced GIT1-Piccolo interactions, showing effects in the order of R299A, F285A, and R298A (the smallest effect observed for R298A). Intriguingly, none of the four mutations appeared to affect the GIT1-βPIX interactions, suggesting the effects of these mutations on GIT1-Piccolo interactions are unlikely to be caused by nonspecific changes in the SHD structure, and that Piccolo and βPIX bind to the SHD of GIT1 by different mechanisms. Introduction of the same mutations to full-length GIT1 gave similar results; the L288A mutation eliminated the GIT1-Piccolo interaction. However, the inhibitory effects of the other mutations on the GIT1-Piccolo interaction were slightly reduced. This could be due to an enhanced affinity between GIT1 and Piccolo in the context of full-length GIT1 (Figs. 1*B* and 2*B*).

We performed coimmunoprecipitation experiments to test whether the same SHD mutations affected biochemical associations of GIT1 with its specific SHD-binding partners (Piccolo, βPIX, and FAK) in heterologous cells (Fig. 5*C*). The L288A mutation in the GIT1 SHD abolished the GIT1-Piccolo association, and the other mutations also reduced GIT1-Piccolo interactions, with effects in the order of R299A ≥ F285A > R298A (Fig. 5*C*, *panel a*), consistent with the yeast two-hybrid results (Fig. 5*B*). However, these mutations did not affect GIT1 coimmunoprecipitation with βPIX (Fig. 5*C*, panel *b*), also consistent with the yeast two-hybrid results (Fig. 5*B*). Intriguingly, all four mutations of the GIT1 SHD eliminated association of GIT1 with FAK, another protein that binds to the GIT1 SHD (25), whereas wild-type GIT1 formed a complex with FAK (Fig. 5*C*, panel *c*). Taken together, these results suggest that Leu-288 of GIT1 plays an important role in binding to Piccolo, and that Piccolo, βPIX, and FAK bind to the SHD of GIT1 by different mechanisms.

GIT Proteins Form Homo- and Heteromultimers through the C-terminal GRKBD—Synaptic multidomain proteins often form multimers (36–39). This organization is thought to be a mechanism for efficiently increasing the complexity of synaptic macromolecular complexes. Because GIT1 is a multidomain protein localized at synaptic sites and it interacts with Piccolo, a potential active zone organizer, we tested whether GIT proteins form multimers. When HEK293T cells doubly transfected with EGFP-GIT1 and GIT1-FLAG or GIT2-FLAG were immunoprecipitated with FLAG antibodies, EGFP-GIT1 coimmunoprecipitated with GIT1-FLAG and GIT2-FLAG (Fig. 6*A*), indicating that GIT proteins can form both homo- and heteromultimers. FLAG antibodies did not bring down EGFP-GIT1 expressed alone (Fig. 6*A*). In the yeast two-hybrid assay, GIT1 and GIT2 interacted with both GIT1 and GIT2 (Fig. 6*B*), confirming the coimmunoprecipitation results (Fig. 6*A*) and indicating that both GIT1 and GIT2 form homo- and heteromultimers.

To determine the minimal region mediating the multimerization, we tested deletions of GIT1 for their ability to form multimers. The C-terminal GRKBD (aa 375–770), but not the N-terminal half (aa 1–374), of GIT1 interacted with full-length GIT1 and GIT2 in the yeast two-hybrid assay (Fig. 6*B*), indicating that the GRKBD mediates homo- and heteromultimerization. In the pull-down assay, a GST fusion protein containing the GRKBD of GIT1 (GST-GRKBD), but not GST alone, brought down EGFP-tagged GIT1 containing the full-length and the GRKBD, but not the N-terminal half (GAP-SHD) (Fig. 6*C*), thus confirming the yeast two-hybrid results (Fig. 6*B*). The limited pull-down of full-length GIT1 by GST-GRKBD as compared with that of the GRKBD may indicate that full-length GIT1 proteins form stronger homomultimers that are less competed for by the shorter construct and, therefore, less efficiently pulled down. GST-GRKBD pulled down H6-GIT1 GRKBD (Fig. 6*D*), indicating that the interaction between GRKBDs is direct. Taken together, these results indicate that GIT proteins form homo- and heteromultimers through a direct interaction between GRKBDs in a tail-to-tail fashion.

The Entire GRKBD Is Involved in Multimerization—The size of the GRKBD is relatively large (~400 aa), and the GRKBD contains several distinct subdomains. The N-terminal region of the GRKBD contains a prominent coiled-coil (CC) domain (aa 432–483) with the properties of a leucine zipper (leucine residues at every seventh aa position). In addition, the C-terminal region of the GRKBD contains paxillin-binding subdomain (PBS, aa 646–770) that is known to associate with paxillin (18, 25). Given this complexity, we sought to further narrow down the minimal region mediating the multimerization. We generated deletions of the GRKBD containing combinations of the CC domain, the PBS domain, and the spacer region in between (termed SP hereafter; aa 486–645) and tested them for binding to full-length GIT1 and GIT2 in the yeast two-hybrid assay. Intriguingly, all the deletions, including the ones containing only the CC domain, the SP region, or the PBS domain, interacted with GIT1 and GIT2 (Fig. 7*A*). Similarly, GST fusion proteins containing only the CC domain, the SP region, or the PBS domain pulled down EGFP-tagged GIT1 GRKBD (Fig. 7*B*). These results indicate that all subregions of the GRKBD participate in the multimerization.

Sedimentation of GIT1 Proteins in a Sucrose Density Gradient Suggests the Formation of Dimers—To determine the stoichiometry of GIT1 multimers, we performed sucrose density

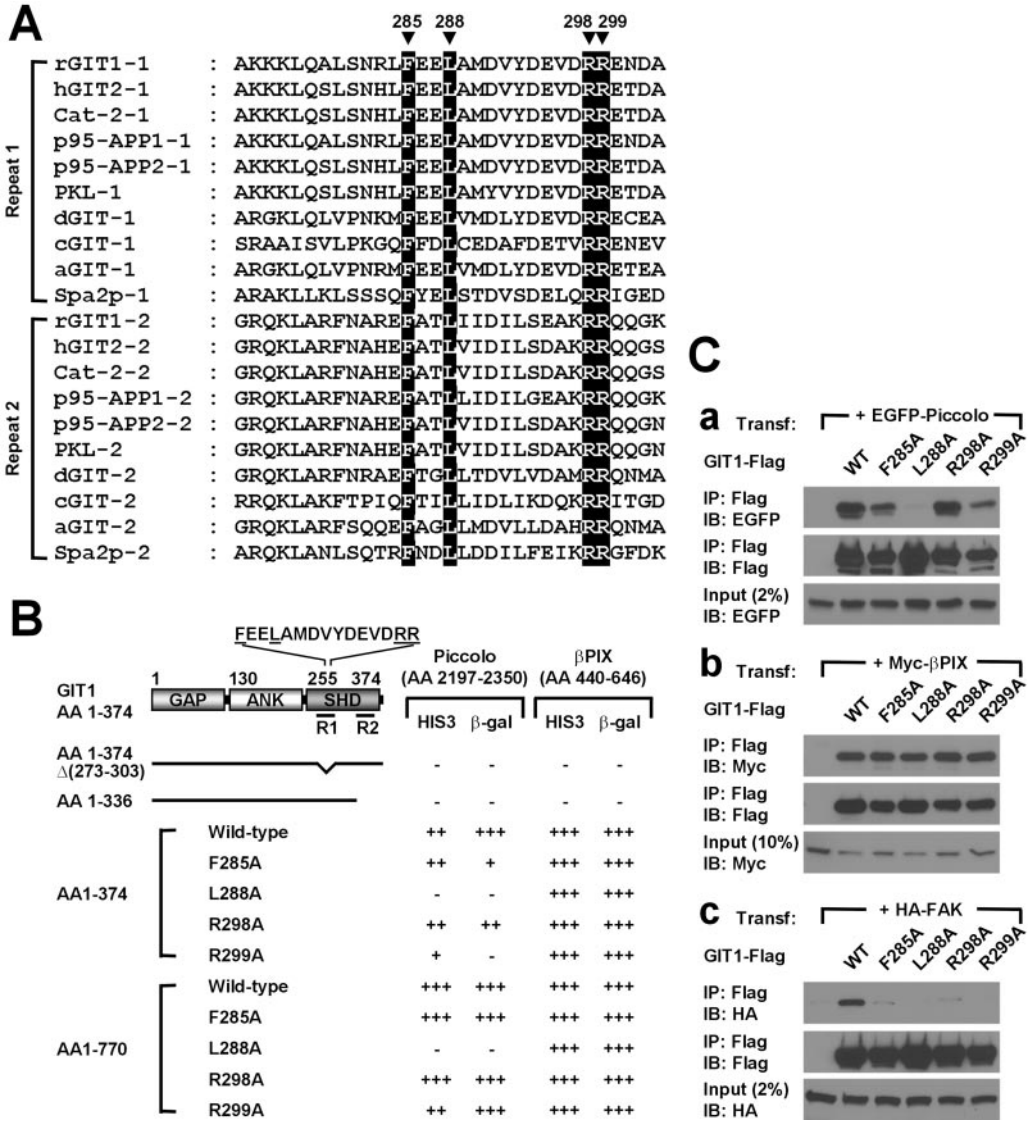

FIG. 5. **Piccolo, βPIX, and FAK bind to the SHD of GIT1 by different mechanisms.** *A*, multiple aa sequence alignment of the two repeats (~30 residues long) in the SHD of GITs from various species and yeast Spa2p. Four invariant residues are indicated by *arrowheads* and *highlighted* as *white characters* in *black boxes*. The residue numbers are from the repeat 1 of rat GIT1. The sources of the aa sequences in the data base are as follows; rGIT1 (AF085693, rat), hGIT2 (NM_057169, human), Cat-2 (AF148693, mouse), p95-APP1 (AF216970, chicken), p95-APP2 (AF134571, chicken), PKL (AF112366, chicken), dGIT (NM_136755, *Drosophila*), cGIT (NM_077360, *C. elegans*), aGIT (EAA03954, *Anopheles*), and Spa2p (NP_013079, yeast). *B*, a yeast-two hybrid assay was used to investigate the effects of deletions and point mutants in the GIT1 SHD (pGAD10) on binding to Piccolo and βPIX (pBHA). *R1*, repeat 1; *R2*, repeat 2. *C*: *panels a–c*, HEK293T cell lysates doubly transfected with GIT1-FLAG mutants plus either EGFP-Piccolo (*a*), Myc-βPIX (*b*), or HA-FAK (*c*) were immunoprecipitated with FLAG antibodies and analyzed by immunoblotting with the indicated antibodies. *Transf*, transfection; *WT*, wild-type.

gradient sedimentation experiments. We employed fusion proteins of H6-GIT1 full-length and H6-GIT1 GAP-SHD (aa 1–374, negative control lacking the GRKBD). Both proteins exhibited a single peak in their sedimentation pattern (Fig. 8, *A* and *B*). When compared with the sedimentation of molecular weight standards (Fig. 8*C*), the peak of H6-GIT full-length corresponded to a molecular mass of 138 kDa, whereas that of H6-GAP-SHD corresponded to 55 kDa, close to its monomeric size (46 kDa). Because the calculated molecular mass of H6-GIT1 full-length is 90 kDa, the size of 138 kDa corresponds to the stoichiometry of 1.53, suggesting that GIT is likely to form dimers. The formation of a single peak of 138 kDa, a size in between monomer and dimer, is likely to be due to incomplete separation monomeric and dimeric peaks.

GIT1 Multimerization Is Required for the Formation of a Ternary Complex between Piccolo, GIT1, and βPIX—Our results and previous reports (16, 18, 25) indicate that Piccolo, βPIX, and FAK bind to the same SHD of GIT1. One of the possible functions of GIT multimerization is to enable GIT proteins to interact with multiple SHD-binding proteins as depicted in Fig. 9*A*. To test this hypothesis, we first attempted to identify smallest possible GIT1 deletions that result in multimerization defects. We generated deletion variants of full-length GIT1 that lacked the CC domain (GIT1 ΔCC; deletion of aa 432–483) and the PBS domain (GIT1 ΔPBS; deletion of aa 646–770) and tested their multimerization by immunoprecipitation experiments. When HEK293T cells doubly transfected with EGFP-GIT1 and GIT1-FLAG (full-length, ΔCC or ΔPBS) were immunoprecipitated with FLAG antibodies, coimmunoprecipitation of EGFP-GIT1 was greatly reduced in GIT1 ΔCC but not in GIT1 full-length or ΔPBS (Fig. 9*B*), indicating that the CC domain is required for GIT multimerization. The slightly smaller effect of CC domain deletion on GIT multimerization in the yeast two-hybrid assay (Fig. 7*A*), compared with that in coimmunoprecipitation experiments, could be due to the deletion of the different regions containing the CC do-

main (aa 432–483 *versus* aa 375–485) or the different size of the backbones for deletion (full-length *versus* the GRKBD) in GIT1-FLAG ΔCC and pGAD10 GIT1 GRKBD (aa 486–770), respectively.

We used this deletion mutant (GIT1 ΔCC) to determine whether GIT1 multimerization is required for the formation of a ternary complex between Piccolo, GIT1, and βPIX. When HEK293T cells triply transfected with EGFP-Piccolo, GIT1-FLAG (full-length or ΔCC), and Myc-βPIX were immunoprecipitated with Myc antibodies, Piccolo was brought down only in the presence of full-length GIT1, but not in the presence of GIT1 ΔCC (Fig. 9*C*). In control experiments, GIT1 ΔCC and full-length GIT1 showed a similar coimmunoprecipitation with Piccolo (Fig. 9*D*) or βPIX (Fig. 9*E*), indicating that the lack of the ternary complex in GIT1 ΔCC (Fig. 9*C*) did not arise from

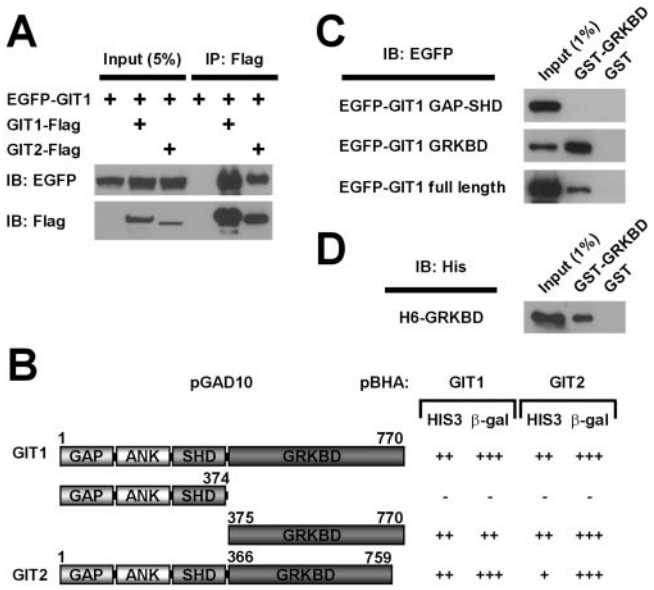

FIG. 6. **GIT family proteins form homo- and heteromultimers through the C-terminal GRKBD.** *A*, HEK293T cell lysates doubly transfected with EGFP-GIT1 and FLAG-tagged GITs (GIT1 or GIT2 long) were immunoprecipitated with FLAG antibodies and analyzed by immunoblotting with EGFP and FLAG antibodies. *B*, GIT1 (full-length and deletions) and GIT2 long in pGAD10 were tested for binding to GIT1 and GIT2 long in pBHA in the yeast two-hybrid assay. *C*, HEK293T cell lysates transfected with EGFP-GIT1 (full-length and deletions) were pulled down by GST-GIT1 GRKBD (*GST-GRKBD*, aa 375–770, 4 μg), or GST alone, and analyzed by immunoblotting with EGFP antibodies. *D*, H6-GIT1 GRKBD fusion proteins (1 μg) were pulled down by GST-GRKBD (2 μg), or GST alone, and analyzed by immunoblotting with His antibodies.

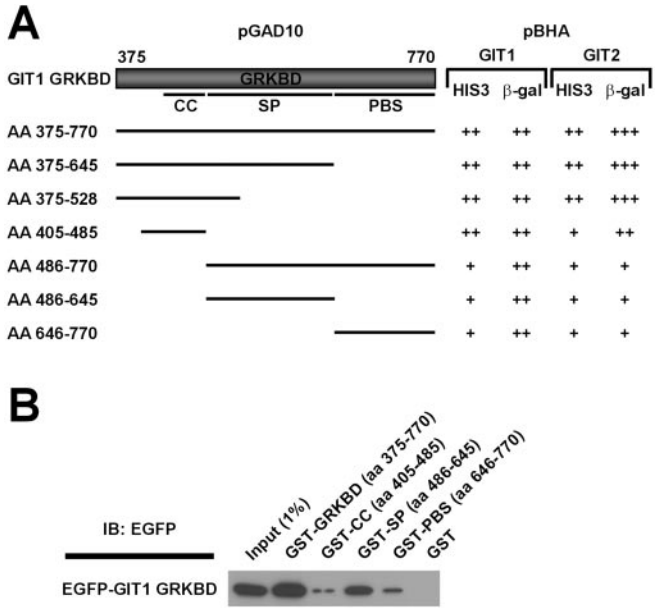

FIG. 7. **The entire GRKBD is involved in multimerization.** *A*, deletions of the GRKBD of GIT1 in pGAD10 were tested for binding to full-length GIT1 and GIT2 in pBHA. *CC*, coiled-coil; *PBS*, paxillin-binding subdomain; *SP*, the spacer region between the CC and PBS domains. *B*, HEK293T cell lysates transiently transfected with EGFP-tagged GIT1 GRKBD were pulled down by GST-GRKBD (aa 375–770), GST-CC (aa 405–485), GST-SP (aa 486–645), GST-PBS (aa 646–770), or GST alone (4 μg each) and analyzed by immunoblotting with EGFP antibodies.

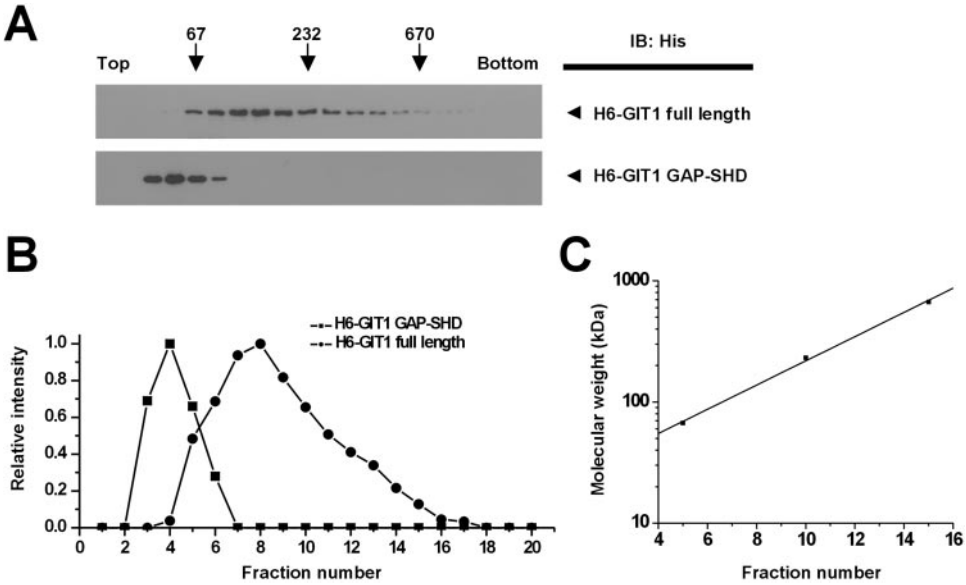

FIG. 8. **Sedimentation of GIT1 in a sucrose density gradient suggests the formation of dimers.** *A*, H6-GIT1 full-length or H6-GIT1 GAP-SHD was sedimented using 15–30% linear sucrose density gradient centrifugation. The molecular mass standards (bovine serum albumin (67 kDa), catalase (232 kDa), and thyroglobulin (670 kDa)) were sedimented in a parallel gradient. Collected fractions were analyzed by immunoblotting using His antibodies. Peak fractions of the standards were determined by Coomassie Brilliant Blue staining. *B*, quantitative analysis of the immunoblot results (*A*). The band intensity in each fraction was normalized to that of the peak fraction. *Closed squares*, H6-GIT1 GAP-SHD; *closed circles*, H6-GIT1 full-length. *C*, sedimentation of molecular weight standards. Molecular weights in log scale were plotted against the number of fractions, followed by linear fitting.

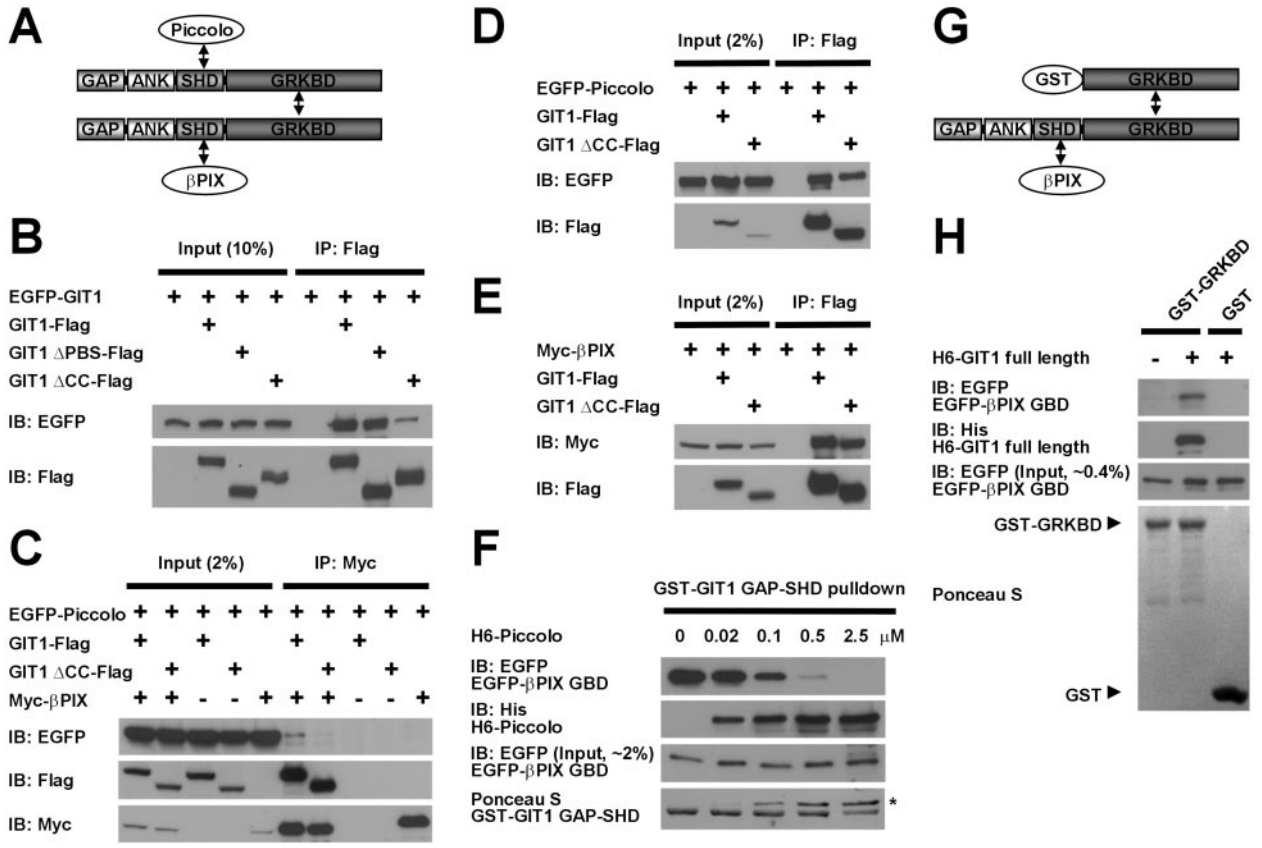

FIG. 9. **GIT multimerization is required for the formation of a ternary complex between Piccolo, GIT1, and βPIX.** *A*, a schematic diagram illustrating the formation of a ternary complex between Piccolo, GIT, and βPIX. *B*, HEK293T cell lysates doubly transfected with EGFP-GIT1 and GIT1-FLAG (full-length, ΔCC, or ΔPBS) were immunoprecipitated with FLAG antibodies and analyzed by immunoblotting with EGFP and FLAG antibodies. *C*, HEK293T cell lysates triply transfected with EGFP-Piccolo, Myc-βPIX, and GIT1-FLAG (full-length or ΔCC) were immunoprecipitated with Myc antibodies and analyzed by immunoblotting with the antibodies indicated. *D* and *E*, HEK293T cell lysates doubly transfected with EGFP-Piccolo plus GIT1-FLAG (full-length or ΔCC), or Myc-βPIX plus GIT1-FLAG (full-length or ΔCC), were immunoprecipitated with FLAG antibodies and analyzed by immunoblotting with the antibodies indicated. *F*, lysates from HEK293T cells transfected with EGFP-βPIX GBD were subjected to pull-down assays using GST-GIT1 GAP-SHD (50 pmol) and increasing amounts of H6-Piccolo. Complexes were analyzed by immunoblotting with EGFP and His antibodies. GST fusion proteins on the membrane were visualized by Ponceau S staining. The *asterisk* indicates H6-Piccolo. *GBD*, GIT-binding domain. *G*, schematic diagram illustrating the formation of a complex containing GST-GIT1 GRKBD, H6-GIT1 full-length, and EGFP-βPIX GBD. *H*, lysates from HEK293T cells transfected with EGFP-βPIX GBD were subjected to pull-down assays using GST-GIT1 GRKBD, or GST alone (6 μg), in the presence or absence of H6-GIT1 full-length (15 μg). Complexes were analyzed by immunoblotting with EGFP and His antibodies. GST fusion proteins on the membrane were visualized by Ponceau S staining.

a reduced binding of GIT1 ΔCC to Piccolo or βPIX. In additional control experiments to support our model, we found that the addition of increasing amounts of H6-Piccolo reduced the pull down of EGFP-βPIX GBD (GIT-binding domain) by GST-GIT1 GAP-SHD (Fig. 9*F*). This indicates that Piccolo and βPIX compete for binding to the GIT1 SHD and suggests that the GIT1 SHD cannot bind two different ligands simultaneously. As an independent way of demonstrating the function of GIT multimerization, we performed the pull-down assay depicted in Fig. 9*G*. GST-GIT1 GRKBD, which cannot pull down EGFP-βPIX by itself, was able to pull down βPIX only in the presence of H6-GIT1 full-length fusion proteins (Fig. 9*H*). Taken together, these results suggest that GIT multimerization is required for the formation of the Piccolo·GIT1·βPIX ternary complex.

DISCUSSION

The molecular mechanisms underlying the organization of the presynaptic CAZ are largely unknown. Our results indicate that the CAZ protein Piccolo associates with GIT proteins as well as various GIT-associated scaffolding and signaling proteins, including liprin-α, βPIX, FAK, and paxillin. Intriguingly, Piccolo, βPIX, and FAK bind to the SHD of GIT1 by different mechanisms. In addition, GIT proteins form homo- and heteromultimers through the GRKBD, and this multimerization enables GIT proteins to simultaneously interact with multiple SHD-binding proteins, including Piccolo and βPIX. These results suggest that GIT proteins, through multimerization and interaction with Piccolo, are involved in organizing the CAZ.

Functions of the Interaction between Piccolo and the GIT Family Proteins—Our data indicate that Piccolo associates with GIT proteins *in vitro* and *in vivo*. A possible function of the Piccolo-GIT interaction can be inferred from their subcellular localizations. Piccolo is restricted to the active zone within the nerve terminal when characterized by immunoelectron microscopic (immuno-EM) analysis (4, 6). Extensive quantitative immuno-EM analysis reveals that GIT1 immunogold particles are sharply concentrated at the active zone in addition to their localization in the postsynaptic density.[2] However, the GIT1 is not confined to synaptic sites. It also shows a widespread distribution to non-synaptic sites as shown by a variety of studies, including immunostaining in cultured neurons, immuno-EM, and subcellular fractionation analysis of rat brain samples.[2] Consistently, GIT1 proteins distribute to several distinct subcellular compartments (adhesion-like structures, the leading edge and cytoplasmic complexes) in non-neuronal cells (40). Thus a reasonable prediction for the function of the Piccolo-GIT interaction based upon the clear difference in their subcellular localizations would be that Piccolo may be involved in the recruitment of GIT proteins to the CAZ.

A possible argument against this hypothesis is that Piccolo and GIT1 may form a complex in the preassembled Piccolo transport vesicle and are inserted together into the plasma membrane of nascent synapses. Zhai *et al.* (2001) showed that Piccolo and other constituents of the active zone such as Bassoon and N-cadherin colocalize in discrete puncta in axonal growth cones of immature cultured neurons (DIV 4). However, we found that Piccolo and GIT1 showed a minimal colocalization in growth cones of immature cultured neurons, whereas we could confirm the reported colocalization between Piccolo and N-cadherin. Thus, it appears that GIT proteins are minimally associated with the preassembled Piccolo transport vesicle and instead associate with Piccolo after the initial formation of the CAZ.

Functions of the GIT Family Proteins in Active Zones—GIT proteins contain various domains for protein interactions as well as an ARF GAP domain. A possible function of GIT proteins would be to bring various GIT-associated proteins to the vicinity of Piccolo. Among the GIT-interacting proteins that we have shown to form a complex with Piccolo (Fig. 4*C*), a protein of particular interest is the multidomain protein liprin-α (41, 42). Mutations in *Dliprin* and *syd-2*, *Drosophila*, and *Caenorhabditis elegans* homologs of liprin-α cause morphological defects in presynaptic active zones (43, 44). In support of the genetic evidence for its presynaptic function, liprin-α associates with the receptor tyrosine phosphatase LAR, a regulator of axon guidance and synaptic target recognition (45–47), and with the active zone scaffolding protein RIM, which regulates neurotransmitter release (8, 48). In addition, liprin-α associates with GRIP/ABP, a family of multi-PDZ domain proteins that interacts with various membrane and signaling proteins, including α-amino-3-hydroxy-5-methyl-4-isoxazole propionic acid glutamate receptors, the RasGEF GRASP-1, and ephrin ligands and their Eph receptors (28, 49–54). Immuno-EM studies indicate that GIT1, liprin-α, and GRIP are localized at the presynaptic nerve terminal in addition to postsynaptic sites (28, 33, 38, 39).[2] Taken together, these results suggest that Piccolo and GIT proteins, in concert with liprin-α and various liprin-α-associated proteins, including LAR, RIM, and GRIP, participate in the organization of the CAZ.

We demonstrated that the GIT family proteins form homo- and heteromultimers through the GRKBD. GIT multimerization is expected to increase the number and diversity of GIT-based docking sites at the active zone. Importantly, Piccolo can from a ternary complex with βPIX through GIT multimers (Fig. 9), suggesting that GIT multimerization may mediate the association of Piccolo with other SHD-binding proteins, including βPIX and FAK. In support of the synaptic function of βPIX, genetic deletion of dPix, a *Drosophila* homolog of βPIX, causes defects in synaptic structure and protein targeting (55). FAK is widely expressed in brain and implicated in the recruitment of various signaling and adaptor proteins, including the Src family of tyrosine kinases (56). Thus βPIX and FAK that are brought to the vicinity of Piccolo through GIT multimers and may participate in the organization of presynaptic active zones. Intriguingly, point mutations in the GIT1 SHD had different effects on the interaction of GIT1 with Piccolo, βPIX, and FAK (Fig. 5), suggesting that Piccolo, βPIX, and FAK bind to the SHD of GIT1 by different mechanisms. Although determination of the exact nature of these differences requires further study, these point mutations may be useful for testing the *in vivo* functional significance of these interactions in future studies.

GIT proteins may exert various presynaptic functions through the modulation of ARF small GTPases. GIT1 regulates endocytosis of various membrane proteins that are internalized by the clathrin-coated pit pathway in a β-arrestin- and dynamin-sensitive manner (15, 24). Importantly, the inhibition of agonist-induced internalization of β_2-adrenergic receptors by GIT1 requires an intact ARF GAP domain (15). ARF6, a substrate of GIT1 (57), is unique among various ARFs in that it regulates actin cytoskeleton rearrangement in various cell types (21, 58–63). ARF6 proteins are expressed in developing hippocampus, and the ARF-specific GEF ARF nucleotide-binding site opener suppresses dendritic branching in cultured hippocampal neurons through ARF6 and Rac1 pathways (64). Consistently, wild-type and truncated GIT1/p95-APP1, through ARF6 and Rac1, induces actin-rich protrusions in fibroblasts (17). Another ARF-specific GEF msec7-1/cytohesin-1 increases neurotransmitter release at the *Xenopus* neuromuscular junction (65). Taken together, these results suggest that GIT proteins, through their ARF modulation, may be involved in the regulation of receptor trafficking, actin cytoskeleton rearrangement, and neurotransmitter release at the active zone.

In conclusion, our results suggest that GIT proteins, through their multimerization and association with Piccolo, contribute to the formation of a Piccolo-based protein network at the active zone. The next step would be to determine how the multifunctional GIT family proteins regulate presynaptic organization and integrate various GIT-associated signaling pathways.

Acknowledgments—We are grateful to Dr. Dongeun Park at Seoul National University for the gift of βPIX expression construct and antibody, Dr. Cheol O. Joe at the Korea Advanced Institute of Science and Technology for FAK expression construct, and Dr. Pann-Ghill Suh at Pohang University of Science and Technology for the GRIP1 (43-8) antibody.

REFERENCES

1. Landis, D. M. (1988) *J. Electron Microsc. Tech.* **10,** 129–151
2. Garner, C. C., Kindler, S., and Gundelfinger, E. D. (2000) *Curr. Opin. Neurobiol.* **10,** 321–327
3. Dresbach, T., Qualmann, B., Kessels, M. M., Garner, C. C., and Gundelfinger, E. D. (2001) *Cell. Mol. Life Sci.* **58,** 94–116
4. Cases-Langhoff, C., Voss, B., Garner, A. M., Appeltauer, U., Takei, K., Kindler, S., Veh, R. W., De Camilli, P., Gundelfinger, E. D., and Garner, C. C. (1996) *Eur. J. Cell Biol.* **69,** 214–223
5. Fenster, S. D., Chung, W. J., Zhai, R., Cases-Langhoff, C., Voss, B., Garner, A. M., Kaempf, U., Kindler, S., Gundelfinger, E. D., and Garner, C. C. (2000) *Neuron* **25,** 203–214
6. Wang, X., Kibschull, M., Laue, M. M., Lichte, B., Petrasch-Parwez, E., and Kilimann, M. W. (1999) *J. Cell Biol.* **147,** 151–162
7. tom Dieck, S., Sanmarti-Vila, L., Langnaese, K., Richter, K., Kindler, S., Soyke, A., Wex, H., Smalla, K. H., Kampf, U., Franzer, J. T., Stumm, M., Garner, C. C., and Gundelfinger, E. D. (1998) *J. Cell Biol.* **142,** 499–509
8. Wang, Y., Okamoto, M., Schmitz, F., Hofmann, K., and Sudhof, T. C. (1997) *Nature* **388,** 593–598
9. Brose, N., Hofmann, K., Hata, Y., and Sudhof, T. C. (1995) *J. Biol. Chem.* **270,** 25273–25280
10. Ohtsuka, T., Takao-Rikitsu, E., Inoue, E., Inoue, M., Takeuchi, M., Matsubara, K., Deguchi-Tawarada, M., Satoh, K., Morimoto, K., Nakanishi, H., and Takai, Y. (2002) *J. Cell Biol.* **158,** 577–590
11. Wang, Y., Liu, X., Biederer, T., and Sudhof, T. C. (2002) *Proc. Natl. Acad. Sci. U. S. A.* **99,** 14464–14469
12. Martincic, I., Peralta, M. E., and Ngsee, J. K. (1997) *J. Biol. Chem.* **272,** 26991–26998
13. Fujimoto, K., Shibasaki, T., Yokoi, N., Kashima, Y., Matsumoto, M., Sasaki, T., Tajima, N., Iwanaga, T., and Seino, S. (2002) *J. Biol. Chem.* **277,** 50497–50502
14. Zhai, R. G., Vardinon-Friedman, H., Cases-Langhoff, C., Becker, B., Gundelfinger, E. D., Ziv, N. E., and Garner, C. C. (2001) *Neuron* **29,** 131–143
15. Premont, R. T., Claing, A., Vitale, N., Freeman, J. L., Pitcher, J. A., Patton, W. A., Moss, J., Vaughan, M., and Lefkowitz, R. J. (1998) *Proc. Natl. Acad. Sci. U. S. A.* **95,** 14082–14087
16. Bagrodia, S., Bailey, D., Lenard, Z., Hart, M., Guan, J. L., Premont, R. T., Taylor, S. J., and Cerione, R. A. (1999) *J. Biol. Chem.* **274,** 22393–22400
17. Di Cesare, A., Paris, S., Albertinazzi, C., Dariozzi, S., Andersen, J., Mann, M., Longhi, R., and de Curtis, I. (2000) *Nat. Cell Biol.* **2,** 521–530
18. Turner, C. E., Brown, M. C., Perrotta, J. A., Riedy, M. C., Nikolopoulos, S. N., McDonald, A. R., Bagrodia, S., Thomas, S., and Leventhal, P. S. (1999) *J. Cell Biol.* **145,** 851–863
19. Premont, R. T., Claing, A., Vitale, N., Perry, S. J., and Lefkowitz, R. J. (2000) *J. Biol. Chem.* **275,** 22373–22380
20. Turner, C. E., West, K. A., and Brown, M. C. (2001) *Curr. Opin. Cell Biol.* **13,** 593–599
21. Donaldson, J. G., and Jackson, C. L. (2000) *Curr. Opin. Cell Biol.* **12,** 475–482
22. Jackson, T. R., Kearns, B. G., and Theibert, A. B. (2000) *Trends Biochem. Sci.*

25, 489–495
23. Chavrier, P., and Goud, B. (1999) *Curr. Opin. Cell Biol.* **11,** 466–475
24. Claing, A., Perry, S. J., Achiriloaie, M., Walker, J. K., Albanesi, J. P., Lefkowitz, R. J., and Premont, R. T. (2000) *Proc. Natl. Acad. Sci. U. S. A.* **97,** 1119–1124
25. Zhao, Z. S., Manser, E., Loo, T. H., and Lim, L. (2000) *Mol. Cell. Biol.* **20,** 6354–6363
26. Kim, E., Niethammer, M., Rothschild, A., Jan, Y. N., and Sheng, M. (1995) *Nature* **378,** 85–88
27. Kim, S., Lee, S. H., and Park, D. (2001) *J. Biol. Chem.* **276,** 10581–10584
28. Wyszynski, M., Valtschanoff, J. G., Naisbitt, S., Dunah, A. W., Kim, E., Standaert, D. G., Weinberg, R., and Sheng, M. (1999) *J. Neurosci.* **19,** 6528–6537
29. Choi, J., Ko, J., Park, E., Lee, J. R., Yoon, J., Lim, S., and Kim, E. (2002) *J. Biol. Chem.* **277,** 12359–12363
30. Dick, O., Hack, I., Altrock, W. D., Garner, C. C., Gundelfinger, E. D., and Brandstatter, J. H. (2001) *J. Comp. Neurol.* **439,** 224–234
31. Goslin, K., and Banker, G. (1991) *Culturing Nerve Cells*, The MIT Press, Cambridge, MA
32. Andreev, J., Simon, J. P., Sabatini, D. D., Kam, J., Plowman, G., Randazzo, P. A., and Schlessinger, J. (1999) *Mol. Cell. Biol.* **19,** 2338–2350
33. Wyszynski, M., Kim, E., Dunah, A. W., Passafaro, M., Valtschanoff, J. G., Serra-Pages, C., Streuli, M., Weinberg, R. J., and Sheng, M. (2002) *Neuron* **34,** 39–52
34. Kim, S., Kim, T., Lee, D., Park, S. H., Kim, H., and Park, D. (2000) *Biochem. Biophys. Res. Commun.* **272,** 721–725
35. Koh, C. G., Manser, E., Zhao, Z. S., Ng, C. P., and Lim, L. (2001) *J. Cell Sci.* **114,** 4239–4251
36. Kim, E., Cho, K. O., Rothschild, A., and Sheng, M. (1996) *Neuron* **17,** 103–113
37. Naisbitt, S., Kim, E., Tu, J. C., Xiao, B., Sala, C., Valtschanoff, J., Weinberg, R. J., Worley, P. F., and Sheng, M. (1999) *Neuron* **23,** 569–582
38. Dong, H., Zhang, P., Song, I., Petralia, R. S., Liao, D., and Huganir, R. L. (1999) *J. Neurosci.* **19,** 6930–6941
39. Srivastava, S., and Ziff, E. B. (1999) *Ann. N. Y. Acad. Sci.* **868,** 561–564
40. Manabe Ri, R., Kovalenko, M., Webb, D. J., and Horwitz, A. R. (2002) *J. Cell Sci.* **115,** 1497–1510
41. Serra-Pages, C., Kedersha, N. L., Fazikas, L., Medley, Q., Debant, A., and Streuli, M. (1995) *EMBO J.* **14,** 2827–2838
42. Serra-Pages, C., Medley, Q. G., Tang, M., Hart, A., and Streuli, M. (1998) *J. Biol. Chem.* **273,** 15611–15620
43. Zhen, M., and Jin, Y. (1999) *Nature* **401,** 371–375
44. Kaufmann, N., DeProto, J., Ranjan, R., Wan, H., and Van Vactor, D. (2002) *Neuron* **34,** 27–38
45. Krueger, N. X., Van Vactor, D., Wan, H. I., Gelbart, W. M., Goodman, C. S., and Saito, H. (1996) *Cell* **84,** 611–622
46. Clandinin, T. R., Lee, C. H., Herman, T., Lee, R. C., Yang, A. Y., Ovasapyan, S., and Zipursky, S. L. (2001) *Neuron* **32,** 237–248
47. Maurel-Zaffran, C., Suzuki, T., Gahmon, G., Treisman, J. E., and Dickson, B. J. (2001) *Neuron* **32,** 225–235
48. Schoch, S., Castillo, P. E., Jo, T., Mukherjee, K., Geppert, M., Wang, Y., Schmitz, F., Malenka, R. C., and Sudhof, T. C. (2002) *Nature* **415,** 321–326
49. Bruckner, K., Pablo Labrador, J., Scheiffele, P., Herb, A., Seeburg, P. H., and Klein, R. (1999) *Neuron* **22,** 511–524
50. Lin, D., Gish, G. D., Songyang, Z., and Pawson, T. (1999) *J. Biol. Chem.* **274,** 3726–3733
51. Torres, R., Firestein, B. L., Dong, H., Staudinger, J., Olson, E. N., Huganir, R. L., Bredt, D. S., Gale, N. W., and Yancopoulos, G. D. (1998) *Neuron* **21,** 1453–1463
52. Ye, B., Liao, D., Zhang, X., Zhang, P., Dong, H., and Huganir, R. L. (2000) *Neuron* **26,** 603–617
53. Dong, H., O'Brien, R. J., Fung, E. T., Lanahan, A. A., Worley, P. F., and Huganir, R. L. (1997) *Nature* **386,** 279–284
54. Srivastava, S., Osten, P., Vilim, F. S., Khatri, L., Inman, G., States, B., Daly, C., DeSouza, S., Abagyan, R., Valtschanoff, J. G., Weinberg, R. J., and Ziff, E. B. (1998) *Neuron* **21,** 581–591
55. Parnas, D., Haghighi, A. P., Fetter, R. D., Kim, S. W., and Goodman, C. S. (2001) *Neuron* **32,** 415–424
56. Girault, J. A., Costa, A., Derkinderen, P., Studler, J. M., and Toutant, M. (1999) *Trends Neurosci.* **22,** 257–263
57. Vitale, N., Patton, W. A., Moss, J., Vaughan, M., Lefkowitz, R. J., and Premont, R. T. (2000) *J. Biol. Chem.* **275,** 13901–13906
58. Radhakrishna, H., Klausner, R. D., and Donaldson, J. G. (1996) *J. Cell Biol.* **134,** 935–947
59. Song, J., Khachikian, Z., Radhakrishna, H., and Donaldson, J. G. (1998) *J. Cell Sci.* **111,** 2257–2267
60. Radhakrishna, H., and Donaldson, J. G. (1997) *J. Cell Biol.* **139,** 49–61
61. Zhang, Q., Cox, D., Tseng, C. C., Donaldson, J. G., and Greenberg, S. (1998) *J. Biol. Chem.* **273,** 19977–19981
62. Al-Awar, O., Radhakrishna, H., Powell, N. N., and Donaldson, J. G. (2000) *Mol. Cell. Biol.* **20,** 5998–6007
63. Frank, S. R., Hatfield, J. C., and Casanova, J. E. (1998) *Mol. Biol. Cell* **9,** 3133–3146
64. Hernandez-Deviez, D. J., Casanova, J. E., and Wilson, J. M. (2002) *Nat. Neurosci.* **5,** 623–624
65. Ashery, U., Koch, H., Scheuss, V., Brose, N., and Rettig, J. (1999) *Proc. Natl. Acad. Sci. U. S. A.* **96,** 1094–1099